Atropselective Oxidation of 2,2',3,3',4,6'-Hexachlorobiphenyl (PCB 132) to Hydroxylated Metabolites by Human Liver Microsomes: Involvement of Arene Oxide Intermediates

Eric Uwimana[a], Xueshu Li[a], Coby Yeung[b], Eric V. Patterson[b] and Hans-Joachim Lehmler[a]

[a]Interdisciplinary Graduate Program in Human Toxicology and Department of Occupational and Environmental Health, College of Public Health, The University of Iowa, Iowa City, Iowa. [b]Department of Chemistry, College of Arts and Sciences, Stony Brook University, Stony Brook, New York.

Corresponding Author:

Dr. Hans-Joachim Lehmler

The University of Iowa

Department of Occupational and Environmental Health

University of Iowa Research Park, B164 MTF

Iowa City, IA 52242-5000

Phone: (319) 335-4981

Fax: (319) 335-4290

e-mail: hans-joachim-lehmler@uiowa.edu

Abstract

PCBs and their hydroxylated metabolites have been associated with neurodevelopmental disorders. Several neurotoxic congeners display axial chirality and atropselectively affect cellular targets implicated in PCB developmental neurotoxicity; however, only limited information is available regarding the metabolism of these congeners in humans. We hypothesize that the oxidation of 2,2',3,3',4,6'-hexachlorobiphenyl (PCB 132) by human liver microsomes (HLMs) is atropselective and displays inter-individual variability. To test this hypothesis, PCB 132 (50 µM) was incubated with pooled or single donor HLMs for 10, 30 or 120 min at 37 °C, and levels and enantiomeric fractions of PCB 132 and its metabolites were determined gas chromatographically. The major metabolite formed by different HLM preparations was either 2,2',3,4,4',6'-hexachlorobiphenyl-3'-ol (3'-140) or 2,2',3,3',4,6'-hexachlorobiphenyl-5'-ol (5'-132). 2,2',3,3',4,6'-Hexachlorobiphenyl-4'-ol (4'-132) and 2,2',3,3',4,6'-hexachlorobiphenyl-4',5'-diol (4',5'-132) were minor metabolites. The second eluting atropisomer of PCB 132 was slightly enriched in some HLM incubations. The formation of the first eluting atropisomer of 3'-140 was nearly enantiospecific (EF > 0.8). The second eluting atropisomer of 5'-132 was enriched in all microsomal preparations investigated. EF values differed slightly between single donor HLM preparations (EF = 0.84 to 0.96 for 3'-140; EF = 0.12 to 0.19 for 5'-132). These findings suggest that there are inter-individual differences in the atropselective biotransformation of PCB 132 to OH-PCBs in humans that may affect neurotoxic outcomes.

Keywords: 1,2-shift, arene oxide, biotransformation, cytochrome P450 enzyme, enantiomers, liver microsomes.

1. Introduction

PCB congeners with a 2,3,6-chlorine substitution pattern on one phenyl ring, such as PCB 132, are important components of commercial PCB mixtures (Kania-Korwel and Lehmler, 2016a). Food is the major source of exposure to these and other PCB congeners (Schecter et al., 2010; Su et al., 2012; Voorspoels et al., 2008). PCB 132 has been detected in fish species caught for human consumption (Wong et al., 2001). Moreover, PCB 132 is present in the indoor air of New York City schools (Thomas et al., 2012), raising concerns about inhalation exposure of school children, teachers and staff to PCB 132 and structurally related PCB congeners (Herrick et al., 2016). Like other PCB congeners with a 2,3,6-chlorine substitution pattern, PCB 132 is axially chiral because it exists as two stable rotational isomers, or atropisomers, which are non-superimposable mirror images of each other (Lehmler et al., 2010). Importantly, chiral PCBs, including PCB 132, are present in human blood (DeCaprio et al., 2005; Jursa et al., 2006; Whitcomb et al., 2005), breast milk (Bordajandi et al., 2008; Bucheli and Brandli, 2006; Glausch et al., 1995) and postmortem human tissue samples (Chu et al., 2003).

Exposure to PCBs has been implicated in the etiology of neurodevelopmental and neurodegenerative disorders (Hatcher-Martin et al., 2012; Jones and Miller, 2008; Pessah et al., 2010). In particular PCB congeners with two or more *ortho* chlorine substituents are neurotoxic and, for example, have been associated with behavioral and cognitive deficits in male mice (Caudle et al., 2006). Similarly, animal studies with hydroxylated PCB metabolites reported impairments in behavioral and locomotor activity in rats and mice (Haijima et al., 2017; Lesmana et al., 2014). Mechanistic studies suggest that these PCBs and, most likely, their metabolites affect the dopaminergic system. In particular *ortho*-chlorinated PCBs inhibited dopamine uptake in rat synaptosomes (Mariussen and Fonnum, 2001) and decreased the dopamine content in cells in culture, possibly due to inhibition of dopamine synthesis (Seegal, 1996). 2,2',3,4',6-Pentachlorobiphenyl (PCB 91) and 2,2',3,5',6-pentachlorobiphenyl (PCB 95) decreased dopamine content in rat synaptosomes by inhibiting vesicular monoamine transporter (VMAT) (Bemis and Seegal, 2004). In contrast, PCB 95 increased intracellular dopamine and decreased

dopamine in medium by down-regulating VMAT2 expression in PC12 cells (Enayah et al., 2018). Striatal dopamine levels in male mice decreased due to a decrease in the expression of dopamine transporter (DAT) and VMAT2 (Richardson and Miller, 2004). Other studies suggest that, in addition to their effects on the dopaminergic system, PCB neurotoxicity can be mediated by altered intracellular Ca^{2+} signaling and/or disruption of thyroid and sex hormone homeostasis (reviewed in (Kodavanti and Curras-Collazo, 2010; Mariussen and Fonnum, 2006; Pessah et al., 2010)).

PCBs are biotransformed to the corresponding hydroxylated metabolites in plants and animals, including humans (Grimm et al., 2015; Kania-Korwel and Lehmler, 2016a). Metabolism of PCBs depends on the number and position of chlorine substituents. Structure-metabolism relationships revealed that PCB congeners with H-atoms in vicinal *meta* and *para* positions are readily metabolized by cytochrome P450 (P450) enzymes, whereas congeners without adjacent *para* and *meta* positions are metabolized more slowly (Grimm et al., 2015). The oxidation of PCBs by P450 enzymes occurs either by direct insertion of an oxygen atom into an aromatic C-H bond or via an arene oxide intermediate (Forgue and Allen, 1982; Forgue et al., 1979; Preston et al., 1983). Several P450 isoforms, including CYP2A and CYP2B enzymes, are involved in the metabolism of *ortho* chlorinated PCB congeners, such as PCB 132, in different species (Lu et al., 2013; McGraw and Waller, 2006; Nagayoshi et al., 2018; Ohta et al., 2012; Waller et al., 1999; Warner et al., 2009). Hydroxylated and methylsulfone metabolites of PCB 132 have been detected in human blood, breast milk and feces (Haraguchi et al., 2004; Haraguchi et al., 2005). Similar to animal studies (Norstroem and Bergman, 2006), PCB 132 undergoes atropisomeric enrichment in humans (Bordajandi et al., 2008; Bucheli and Brandli, 2006; Chu et al., 2003; Glausch et al., 1995; Zheng et al., 2016). These non-racemic chiral signatures of PCB 132 are most likely due to the atropselective metabolism of racemic PCB 132 to hydroxylated and other metabolites by P450 enzymes.

Several biotransformation studies reveal species differences in the metabolism of PCBs to chiral hydroxylated metabolites (Kania-Korwel and Lehmler, 2016a); however, only a few studies of the

93 metabolism of PCBs in humans have been reported to date (Schnellmann et al., 1983; Uwimana et al.,
94 2016, 2018; Wu et al., 2014). Because of the growing evidence that OH-PCB are present in the
95 environment (Tehrani and Van Aken, 2014) and represent an environmental and human health concern
96 (Grimm et al., 2015; Kania-Korwel and Lehmler, 2016a), the objective of this study was to investigate
97 the atropselective metabolism of PCB 132 to OH-PCB metabolites by HLMs.
98
99 **2. Materials and Methods**
100 *2.1. Chemicals and materials*
101 Sources and purities of racemic PCB 132 (**Table S1**), PCB metabolite standards, chemicals and
102 other reagents; information regarding the HLM preparations; and a description of the separation and
103 characterization of PCB 132 atropisomers are presented in the Supplementary Material. Gas
104 chromatograms and the corresponding mass spectrum of PCB 132 are shown in **Figs. S1** and **S2**. The
105 chemical structures and abbreviations of OH-PCB 132 metabolites are shown in **Fig. 1**.
106
107 *2.2. Microsomal incubations*
108 The metabolism of PCB 132 was investigated in incubations containing sodium phosphate buffer
109 (0.1 M, pH 7.4), magnesium chloride (3 mM), pooled human liver microsomes (pHLMs) or single
110 donor HLMs (0.1 mg/mL), and NADPH (1 mM) as described previously (Kania-Korwel et al., 2011;
111 Uwimana et al., 2017; Wu et al., 2011). Following a 5 min preincubation, PCB 132 (50 µM in DMSO; ≤
112 0.5% *v/v*) was added to the incubation system (2 mL final volume). The mixtures were incubated for 10,
113 30 or 120 min at 37°C. Incubations with (-)-PCB 132, (+)-PCB132 or racemic PCB 132 (50 µM in
114 DMSO; ≤ 0.5% *v/v*) were carried out analogously for 30 min at 37°C. The formation of PCB 132
115 metabolites was linear with time for up to 30 min. To terminate the enzymatic reaction, ice-cold sodium
116 hydroxide (2 mL, 0.5 M) was added to each sample and the incubation mixtures were heated at 110 °C
117 for 10 min. Phosphate buffer blanks and control incubations without PCB accompanied each

118 microsomal preparation. To control for abiotic transformation of PCB 132, the following incubations
119 were performed in parallel with each metabolism study: (1) without NADPH, (2) without microsomes,
120 and (3) heat inactivated microsomes. No metabolites were detected in any of the control samples. If not
121 stated otherwise, incubations with HLMs were performed in triplicate.
122
123 *2.3. Extraction of hydroxylated PCB 132 metabolites*
124 PCB 132 and its hydroxylated metabolites were extracted from the incubation mixtures as
125 reported previously (Kania-Korwel et al., 2011; Uwimana et al., 2016; Wu et al., 2011). Briefly,
126 samples were spiked with PCB 117 (200 ng) and 4'-159 (68.5 ng) as recovery standards. Hydrochloric
127 acid (6 M, 1 mL) was added, followed by 2-propanol (5 mL). The samples were extracted with hexane-
128 MTBE (1:1 *v/v*, 5 mL) and re-extracted with hexane (3 mL). The combined organic layers were washed
129 with an aqueous potassium chloride solution (1%, 4 mL), the organic phase was transferred to a new
130 vial, and the KCl mixture was re-extracted with hexane (3 mL). The combined organic layers were
131 evaporated to dryness under a gentle stream of nitrogen. The samples were reconstituted with hexane (1
132 mL), derivatized with diazomethane in diethyl ether (0.5 mL) for approximately 16 h at 4 °C (Kania-
133 Korwel et al., 2008), and underwent sulfur and sulfuric acid clean-up steps prior to gas chromatographic
134 analysis (Kania-Korwel et al., 2005; Kania-Korwel et al., 2007).
135
136 *2.4. Identification of PCB 132 metabolites*
137 High resolution gas chromatography with time-of-flight mass spectrometry (GC/TOF-MS) was
138 used to confirm the identity of the hydroxylated metabolites formed in incubations of PCB 132 with
139 pHLMs as described (Uwimana et al., 2016, 2018). To obtain metabolite levels sufficient for GC/TOF-
140 MS analysis, incubations were performed using the following experimental conditions: 50 µM racemic
141 PCB 132, 0.3 mg/mL microsomal protein and 1 mM NADPH for 90 min at 37 °C. Metabolites were
142 extracted and derivatized as described above, and samples were analyzed on a Waters GCT Premier gas

chromatograph (Waters Corporation, Milford, MA, USA) combined with a time-of-flight mass spectrometer in the High-Resolution Mass Spectrometry Facility of the University of Iowa (Iowa City, IA, USA). Methylated PCB 132 metabolites were separated on a DB-5ms column (30 m length, 250 µm inner diameter, 0.25 µm film thickness; Agilent, Santa Clara, CA, USA). Details regarding the instrument parameters have been described previously (Uwimana et al., 2016, 2018). Analyses were carried out in the presence and in the absence of heptacosafluorotributylamine as internal standard (lock mass) to determine the accurate mass of $[M]^+$ and obtain mass spectra of the metabolites, respectively. Metabolites were identified with the following criteria: The average relative retention times (RRT) (n=3) of the metabolites, calculated relative to PCB 51 as internal standard, were within 0.5% of the RRT of the respective authentic standard (European Commission, 2002); experimental accurate mass determinations were within 0.003 Da of the theoretical mass of $[M]^+$; and the isotope pattern of $[M]^+$ matched the theoretical abundance ratios of hexachlorinated biphenyl derivatives within a 20 % error.

2.5. Quantification of PCB 132 metabolite levels

Levels of OH-PCB 132 metabolites (as methylated derivatives) in extracts were quantified on an Agilent 7890A gas chromatograph with a ^{63}Ni-micro electron capture detector (µECD) and a SPB-1 capillary column (60 m length, 250 µm inner diameter, 0.25 µm film thickness; Supelco, St Louis, MO, USA) as reported earlier (Uwimana et al., 2016; Uwimana et al., 2017; Wu et al., 2013b). PCB 204 was added as internal standard (volume corrector) prior to analysis, and concentrations of OH-PCB 132 metabolites (as methylated derivatives) were determined using the internal standard method (Kania-Korwel et al., 2011; Wu and Lehmler, 2016; Wu et al., 2011). Levels of PCB and its metabolites were not adjusted for recovery to facilitate a comparison with earlier studies (Uwimana et al., 2016, 2018; Wu and Lehmler, 2016). The average RRTs of the metabolites, calculated relative to PCB 204, were within 0.5% of the RRT for the respective standard (European Commission, 2002). Metabolite levels

and formation rates for all experiments described in the manuscript are summarized in the Supplementary Material (**Tables S2-S4**).

2.6. Ring opening calculations

The ring opening reactions were modeled using density functional theory at the M11/def2-SVP level of theory (Peverati and Truhlar, 2011; Weigend and Ahlrichs, 2005), coupled with the SMD aqueous continuum solvation model (Marenich et al., 2009). The reactions were examined under neutral conditions, with two explicit water molecules complexed to the system to serve as a proton shuttle. To ascertain steric and electronic effects, calculations were carried out on epoxides formed from 1,2,4-trichlorobenzene (TCB), 1,2,4-trichlorobiphenyl (TCP), PCB 91, PCB 95, PCB 132, and PCB 136. Transition states were characterized by normal mode analysis and confirmed via IRC calculations. All calculations were performed using Gaussian 16, Rev. A.01 (Frisch et al., 2016). Additional details including computational data are available in the Supplementary Material.

2.7. Atropselective analyses

Atropselective analyses were carried out with extracts from long-term incubations (*i.e.*, 5 or 50 µM PCB 132, 120 minutes at 37 ºC, 0.5 mg/mL protein, and 0.5 mM NADPH) and extracts from the 30 min incubations described above. Hydroxylated metabolites were analyzed as methylated derivatives after derivatization with diazomethane. Analyses were performed on an Agilent 6890 gas chromatograph equipped with a µECD detector and a CP-Chirasil-Dex CB (CD) (25 m length, 250 µm inner diameter, 0.12 µm film thickness; Agilent, Santa Clara, CA, USA) or a ChiralDex G-TA (GTA) capillary column (30 m length, 250 µm inner diameter, 0.12 µm film thickness; Supelco, St Louis, MO, USA) (Kania-Korwel et al., 2011; Uwimana et al., 2017). The following temperature program was use for the atropselective analysis of PCB 132 and 5'-132 on a CD column: initial temperature was 50 °C held for 1 min, ramped at 10 °C/min to 160 °C and held for 220 min, the temperature was then ramped

192 at 20 °C/min to the final temperature of 200 °C and held for 10 min. To analyze 3'-140 on a GTA
193 column, the temperature program was as follows: initial temperature was 50 °C held for 1 min, ramped
194 at 10 °C/min to 150 °C and held for 400 min, the temperature was then ramped at 10 °C/min to the final
195 temperature of 180 °C and held for 40 min. The helium flow was 3 mL/min. To facilitate a comparison
196 with earlier studies (Kania-Korwel and Lehmler, 2016b; Uwimana et al., 2016; Uwimana et al., 2017;
197 Wu et al., 2011), enantiomeric fractions (EFs) were calculated by the drop valley method (Asher et al.,
198 2009) as EF = Area E_1/(Area E_1 + Area E_2), were Area E_1 and Area E_2 denote the peak area of the first
199 (E_1)and second (E_2) eluting atropisomer on the respective column. All EF values are summarized in the
200 Supplementary Material (**Table S6**).
201
202 *2.8. Quality Assurance and Quality Control*
203 The response of the µECDs used in this study was linear for all analytes up to concentrations of
204 1,000 ng/mL ($R^2 \geq 0.999$). The recoveries of PCB 117 were 93 ± 13% (n = 120). Recoveries of 4'-159
205 could not be determined due to co-elution with 4',5'-132. The limits of detection (LOD) of the PCB 132
206 metabolites were calculated from blank buffer samples as LOD = mean of blank samples + k * standard
207 deviation of blank samples, where k is the student's t value for a degree of freedom n-1 = 5 at 99%
208 confidence level) (Kania-Korwel et al., 2011; Uwimana et al., 2016; Wu and Lehmler, 2016; Wu et al.,
209 2011). The LODs were 0.03, 0.1 and 0.21 ng for 3'-140, 5'-132 and 4'-132, respectively. The
210 background levels for 3'-140, 5'-132 and 4'-132 in control (DMSO) incubations with HLMs (n=6) were
211 0.17, 0.13 and 0.19 ng, respectively. The resolution of the atropisomers of PCB 132 and 5'-132 on the
212 CD column was 1.05 and 2.02, respectively. The resolution of the atropisomers of 3'-140 on the GTA
213 column was 1.18. The EF values of the racemic standards of PCB 132, 3'-140 and 5'-132 were 0.51 ±
214 0.01 (n=2), 0.50 ± 0.01 (n=3) and 0.49 ± 0.01 (n=3), respectively. The data are presented as the mean ±
215 standard deviation.
216

3. Results and discussion

3.1. Identification and quantification of PCB 132 metabolites in incubations with pHLMs

Several human biomonitoring studies have reported an atropisomeric enrichment of PCB 132 in human samples (**Table S8**) (Lehmler et al., 2010); however, the atropselective oxidation of this PCB congener to hydroxylated metabolites by HLMs has not been studied to date (Grimm et al., 2015; Kania-Korwel and Lehmler, 2016a). Our GC/TOF-MS analyses revealed the formation of three monohydroxylated and one dihydroxylated PCB metabolite in incubations of racemic PCB 132 with pHLMs (**Fig. 2; Figs. S4-S11**). The structure of these metabolites is shown in the simplified metabolism scheme in **Fig. 1**. Their identification was based on accurate mass determinations, the chlorine isotope patterns of their molecular ion (analyzed as methylated derivatives) and their fragmentation patterns; for additional discussion, see the Supplementary Material. PCB 132 was oxidized by pooled and individual donor HLMs in the *meta* position, with 5'-132 and 3'-140, a 1,2-shirt product, being major metabolites (**Figs. 3-4; Table S2**). 4'-132 was only a minor metabolite. 4',5'-132 could not be quantified in this study due to co-elution with the recovery standard, 4'-159; however, this metabolite was only a minor metabolite.

It is noteworthy that 3'-140, one of the major metabolites observed in all HLM preparations, is a 1,2-shift product (Guroff et al., 1967) that is formed *via* an arene oxide intermediate, followed by a 1,2-shift of the 3'-chlorine substituent to the *para* position. In contrast, *in vitro* studies consistently show that 5'-132 is a major metabolite of PCB 132 in rodents. For example, 5'-132 was the major metabolite formed in experiments with rat liver microsomes (Kania-Korwel et al., 2011), recombinant rat CYP2B1 (Lu et al., 2013), and precision-cut mouse liver tissue slices (Wu et al., 2013a). 1,2-Shift products are only minor metabolites of PCB 132 and other chiral PCBs in *in vitro* and *in vivo* studies in rodent models (Kania-Korwel et al., 2011; Lu et al., 2013; Wu et al., 2013a). Analogous to the structurally related PCB 52 (Preston et al., 1983), oxidation of the *meta* position of PCB 132 to 5'-132 by rat CYP2B1 is thought to occur via a direct insertion of an oxygen atom into an aromatic C-H bond.

Another important observation is that PCB 132 was oxidized by HLMs in the 2,3,6-trichloro substituted ring, whereas no oxidation was observed in the 2,3,4-chloro substituted ring. This observation is consistent with earlier reports that *ortho* substituted PCBs with a *para* chlorine substituent in one phenyl ring are preferentially oxidized by rat (Kennedy et al., 1981) and human enzymes (Uwimana et al., 2018) in the non-*para* substituted ring. Moreover, the oxidation of PCB 132 in positions with vicinal H substituents in *meta-para* positions is consistent with published structure-metabolism relationships of PCBs (Kannan et al., 1995).

3.2. Congener specific metabolism of ortho substituted PCBs by HLMs

A comparison of the PCB 132 metabolite profiles formed by HLMs with the metabolite profiles of structurally related PCB congeners with a 2,3,6-trichlorophenyl group (*i.e.*, PCB 91, PCB 95 and 2,2',3,3',6,6'-hexachlorobiphenyl [PCB 136]) reveals considerable congener-specific differences in the regioselectivity of the P450 enzyme-mediated oxidation of PCBs (**Fig. 4a**). In this study, PCB 132 was oxidized by HLMs in the *meta* position to yield the 1,2-shift product, 3'-140, and 5'-132. PCB 91, which is structurally similar to PCB 132, was also primarily metabolized to a 1,2-shift product by HLMs; however, the corresponding 5-91 metabolite was only a minor metabolites (Uwimana et al., 2018). In contrast to PCB 132 and PCB 91, PCB 95 was preferentially oxidized by HLMs in the *para* position with the lower chlorinated, 2,5-dichloro substituted phenyl ring, and only traces of a 1,2-shift product were formed by with different HLM preparations (Uwimana et al., 2016). PCB 136 was metabolized in both the *meta* and *para* position to yield comparable levels of 5'-136 and 4'-136, with ratios of 5'-136: 4'-136 of 0.4 to 0.8:1 and 1.3:1 reported for different HLM preparations (Schnellmann et al., 1983; Wu et al., 2014).

To assess if congener-specific differences in OH-PCB metabolite profiles are due to different arene oxide intermediates and/or different substitution pattern in the second phenyl ring of chiral PCB congeners, the energetics of different arene oxide ring opening reactions were determined for 1,2,4-

trichlorobenzene, 2,3,6-trichlorobiphenyl, PCB 91, PCB 95, PCB 132, and PCB 136 (**Figs. 5 and S12, Table S5**). The 3,4- , 4,5-, and 5,6-arene oxides of PCB 132 and PCB 136 were found to be essentially isoenergetic, lying within ±2 kcal/mol of each other. Differences due to atopisomerism are also negligible within ±1 kcal/mol. Therefore, in the absence of a chiral environment, we predict no inherent factors to favor the formation of an arene oxide regioisomer or arene oxide atropisomer over another. Only the 3,4-arene oxides were explored for the other compounds.

Complete ring-opening pathways were computed for the 3,4-, 4,5-, and 5,6-arene oxides for a single atropisomer of PCB 132. In addition, the ring opening pathways were investigated for PCB 136, a well-investigated chiral PCB congener. As each epoxide may open either of two directions, six pathways were computed for PCB 132 and PCB 136. In the case of the 3,4- (and 5,6-) arene oxide, the arene oxide opening towards the C-Cl group and the 1,2-shift of the chlorine were concerted, with barriers to opening of approximately 25 kcal/mol (**Fig. S12**). The proton transfer step to form the phenol and restore aromaticity proceeded with a negligible barrier and was essentially spontaneous.

In contrast, when the 3,4- (and 5,6-) arene oxides open towards the aromatic C-H bond, the energy barrier to arene oxide opening was approximately 40 kcal/mol for both arene oxides (**Fig. 5**). For both the 3,4- and 5,6-arene oxides, this mode of opening leads to formation of the 4,5-arene oxide as confirmed by IRC calculations. Therefore, ring opening of the 4,5-arene oxides was also modeled. As both possible openings of the 4,5-arene oxide proceed towards C-H, it is not surprising that the barriers were found to also be approximately 40 kcal/mol. Here, IRC calculations do reveal concerted 1,2-hydride shifts analogous to the 1,2-chloride shift observed for 3,4-arene oxide opening toward C-Cl.

Partial pathways opening toward C-Cl were explored for the 3,4-arene oxides of 1,2,4-trichlorobenzene, 2,3,6-trichlorobiphenyl, PCB 91 and PCB 95. The presence or absence of the substituent aryl ring had no effect on the computed mechanism or energetics for opening toward C-Cl, nor did the substitution pattern on the aryl substituent. For 1,2,4-trichlorobenzene, ring opening in the C-H direction was also modeled. It was found that the 3,4-arene oxide to 4,5-arene oxide rearrangement

mentioned above does not exist for 1,2,4-trichlorobenzene. Instead, a 1,2-hydride shift is predicted. However, the energetics are not affected by this variation in the mechanism.

We therefore conclude that the presence of the second aromatic ring does not perturb the energetics relative to the simplest case, 1,2,4-trichlorobenzene, an observation that applies to all PCB congeners of interest (**Table S5**). This is in contrast to computational results reported by Kaminsky et al. on dichlorobiphenyls (Kaminsky et al., 1981). However, their results relied on constrained optimizations at the semiempirical MNDO level of theory and cannot be considered reliable by current standards. Nevertheless, we do find agreement that the 3,4-arene oxide is the most likely intermediate leading to major products. Thus, we conclude that the 1,2-chloride shift products, major metabolites of both PCB 132 (this study) and PCB 91 (Uwimana et al., 2018), are formed via an 3,4-arene oxide intermediate which opens toward C-Cl, with no significant influence from the second aromatic ring. The absence of an *ortho* substituted 1,2-shift product in incubations of PCB 132 and other chiral PCBs with HLMs suggests that the corresponding 5,6-arene oxides are probably not formed by human P450 enzymes. The present study also indicates that the formation of *para* substituted metabolites of PCB 95 and PCB 136 is not simply due to the energetically favored opening of an arene oxide intermediate. Instead, congener specific differences in the steric or electronic interaction of chiral PCBs, such as PCB 132, with specific P450 isoforms likely affect the rearrangement of the arene oxide intermediates to OH-PCBs.

3.3. Inter-individual differences in PCB 132 metabolism by HLMs

In experiments with single donor HLMs, the formation rates of the monohydroxylated PCB 132 metabolites displayed inter-individual variation (**Figs. 3** and **4b; Tables S3** and **S4**). This is not surprising considering the well documented variability of P450 enzyme activities among humans (Guengerich, 2015). The sum of OH-PCBs (ΣOH-PCBs) formed by single donor HLM preparations followed the following rank order: donor H5 > H4 ~ H3 > H2 ~ pHLM > H1. Notably, levels of ΣOH-PCB were 4.5-fold higher in incubations with HLMs from donors H5 *vs.* H1. The rate of 5'-132

formation differed 16-fold for incubations with HLM preparations from donors H1 *vs.* H4. The rate of 3'-140 and 4'-132 formation differed 2.2 and 3.3-fold, respectively, for incubations with HLM preparations from donors H1 *vs.* H5. As a consequence, the OH-PCB metabolite profiles differed across the HLM preparations investigated (**Fig. 4b**). Briefly, 3'-140 and 5'-132 were formed in a 1:1 ratio by pHLMs. In incubations with HLMs from donors H1 and H2, the 3'-140 to 5'-132 ratios were 3.9:1 and 1.4:1 for donors H1 and H2, respectively. In contrast, 5'-132, and not 3'-140, were major in incubations with HLMs from donors H3, H4 and H5 (3'-140 to 5'-132 ratios were 0.7:1, 0.3:1 and 0.6:1 for donors H3, H4 and H5, respectively). Although only a small number of single donor HLM preparations were investigated in this and other studies, the profiles of OH-PCB metabolite formed in the liver likely display considerable variability in humans.

3.4. Atropisomeric enrichment of PCB 132

Because chiral PCBs affect toxic endpoints in an atropselective manner, the enrichment of PCB 132 atropisomers in incubations of racemic PCB 132 with HLMs was investigated with atropselective gas chromatography. E_2-PCB 132 (EF = 0.39), which corresponds to (+)-PCB 132 (Haglund and Wiberg, 1996), was enriched in experiments with low PCB 132 concentration (5 µM) and long incubation time (120 min) (**Fig. 6**, **Table S6**). EF values were near racemic in incubations with higher PCB 132 concentrations (50 µM) because the large amount of racemic PCB 132 masked the atropselective depletion of one PCB 132 atropisomer over the other (Uwimana et al., 2016, 2018). Several small human biomonitoring studies also observed an enrichment of (+)-PCB 132 in human tissues and biospecimen samples, with EF values of PCB 132 ranging from 0.18 to 0.48 in breast milk and 0.32 to 0.49 in liver (**Table S8**). A single brain tissue sample from Belgium showed an enrichment of (-)-PCB 132 (Chu et al., 2003). PCB 132 was racemic in human hair (Zheng et al., 2013; Zheng et al., 2016), but displayed an enrichment of (-)-PCB 132 (EF = 0.55 ± 0.06) in serum from Chinese e-waste recycling workers (Zheng et al., 2016).

342 In animal studies, (+)-PCB 132 was enriched in female mice (Kania-Korwel et al., 2010;
343 Milanowski et al., 2010), male Wistar rats (Norstrom et al., 2006), bivalves (Wong et al., 2001) and
344 plants *in vivo* (Chen et al., 2014). (-)-PCB 132 had a shorter half-life in a disposition study in mice
345 (Kania-Korwel et al., 2010). (+)-PCB 132 was also enriched in *in vitro* metabolism studies with
346 precision-cut mouse liver tissue slices (Wu et al., 2013a), rat liver microsomes (Kania-Korwel et al.,
347 2011), and recombinant rat CYP2B1 and human CYP2B6 (Lu et al., 2013; Warner et al., 2009). Active
348 transporters, such as Mdr1a/b, did not contribute to the atropisomeric enrichment of chiral PCBs, such
349 as PCB 132, in mice (Milanowski et al., 2010). Taken together, the enrichment of PCB atropisomers
350 observed in *in vitro* studies appears to predict the atropisomeric enrichment observed in animal studies.
351 Analogously, our findings strongly suggest that the enrichment of (+)-PCB 132 observed in most human
352 samples (**Table S8**) is due to the preferential biotransformation of (-)-PCB 132 to OH-PCBs and other
353 metabolites. In addition, exposure to atropisomerically enriched PCB 132 *via* the diet may also
354 contribute to the atropisomeric enrichment of PCB 132 in humans (Harrad et al., 2006; Vetter, 2016).
355 Because our study was not designed to quantify levels of PCB 132 metabolites formed *via* arene oxide
356 intermediates, additional studies are needed to demonstrate that *in vitro* metabolism studies are indeed
357 predictive of chiral signatures of PCB 132 in human samples.
358
359 *3.5. Atropselective formation of OH-PCB 132 metabolites*
360 Several studies have reported the atropselective formation of chiral OH-PCB metabolites, both
361 from chiral and prochiral PCBs, in *in vitro* and *in vivo* studies (Kania-Korwel and Lehmler, 2016a;
362 Lehmler et al., 2010; Uwimana et al., 2017). Consistent with these earlier studies, we observed the
363 atropselective formation of different OH-PCB 132 metabolites in incubations with HLMs. Specifically,
364 the atropselective analysis on the GTA column revealed the atropselective formation of E_1-3'-140, with
365 EF values > 0.8 (range: 0.84 to 0.95) (**Figs. 6-7**). E_1-3'-140 was also enriched in experiments with rat
366 liver microsomes (Kania-Korwel et al., 2011). E_2-5'-132 was significantly enriched with EF values < 0.2

(range: 0.12 to 0.18) in incubations with HLMs. Similarly, metabolism of racemic PCB 132 resulted in an enrichment of E_2-5'-132 in incubations with rat liver microsomes (Kania-Korwel et al., 2011) and mouse live tissue slices (Wu et al., 2013a). In contrast, rat CYP2B1 metabolized PCB 132 preferentially to E_1-5'-132, which indicates the involvement of other P450 isoforms in the atropselective oxidation of PCB 132 in incubations with rat liver microsomes (Lu et al., 2013). As reported previously, the atropisomers of 4-132 could not be resolved on any of the chiral columns used (Kania-Korwel et al., 2011).

To determine which of E_1-OH-PCB and E_2-OH-PCB atropisomer is formed from (-)- or (+)-PCB 132, we investigated the metabolism of (-)-, (±)-, and (+)-PCB 132 by pHLMs (**Fig. 8**, **Table S7**). The atropselective analysis showed that E_1-5'-132 is formed from (+)-PCB 132. Conversely, E_1-3'-140 and E_2-5'-132 are formed from (-)-PCB 132. The ΣOH-PCBs formed from (-)-PCB 132 was 3-times the ΣOH-PCBs formed from (+)-PCB 132 (**Table S7**). A more complex picture emerges when individual OH-PCB 132 metabolites are analyzed (**Figs. 8e-g**). The levels of both major metabolites, 3'-140 and 5'-132, decreased in the order of (-)-PCB 132 > (±)-PCB 132 > (+)-PCB 132. In contrast, levels of the minor metabolite, 4'-132, decreased in the reverse order. As a consequence, the OH-PCB 132 metabolite profiles formed by HLMs differ considerably for incubations with (-)-, (±)-, and (+)-PCB 132 (**Fig. 8h**). Overall, the faster metabolism of (-)-PCB 132 to OH-PCBs is consistent with the enrichment of (+)-PCB 132 in incubations of racemic PCB 132 with pHLMs (**Fig. 6a2**) and the enrichment of (+)-PCB 132 in most human tissue samples (**Table S8**). Consistent with our results, levels of methyl sulfone metabolites of PCB 132 were higher in rats exposed to (-)-PCB 132 compared to rats exposed to (+)-PCB 132, suggesting that (-)-PCB 132 is more rapidly metabolized in rats (Norstrom et al., 2006).

3.6. Implications for ecosystem and environmental health

Biotransformation of chiral PCBs results in non-racemic chiral signatures of parent PCBs and their metabolites in environmental samples, including wildlife, livestock, plants and humans (Kania-

392 Korwel and Lehmler, 2016b; Lehmler et al., 2010). The atropisomeric enrichment of chiral PCBs and
393 chiral metabolites is concerning because chiral PCBs may have atropselective toxic effect. Several
394 studies show atropselective biological effects of pure PCBs atropisomers. PCB atropisomers have
395 different effects on the expression and activity of xenobiotic processing genes (Parkinson et al., 1983;
396 Pencikova et al., 2018; Safe et al., 1985). For example, chiral PCBs atropselectively induce P450
397 enzymes, with penta- and hexachlorinated PCBs being more active than octachlorinated PCBs in rats
398 (Püttmann et al., 1990; Püttmann et al., 1989) and in chick hepatocyte cultures (Rodman et al., 1991),
399 most likely due to atropselective interaction with nuclear receptors, such as pregnane X receptor (PXR)
400 and constitutive androstane receptor (CAR), that regulate the expression of hepatic P450 enzymes
401 (Gährs et al., 2013). In the human HepaRG cell line, (-)-PCB 136 activated PXR and CAR to a greater
402 extent than (+)-PCB 136, as inferred from the atropselective induction of the expression of CYP2B6 and
403 CYP3A4 (Pencikova et al., 2018).

404 Chiral PCBs also affect endpoints implicated in PCB developmental neurotoxicity in an
405 atropselective manner. For example (-)-PCB136, but not (+)-PCB 136 is a potent sensitizer of ryanodine
406 receptors (RyRs) and affects dendritic growth and neuronal connectivity via a calcium-dependent
407 mechanism involving RyRs (Yang et al., 2014). Similarly, (-)-PCB 95 showed greater RyR1 binding
408 and an increased rate of calcium efflux relative to (+)-PCB 95 in skeletal muscle (Feng et al., 2017). In
409 the same study, (+)-PCB 95 had a slightly stronger effect on mixtures of RyRs present in the brain and
410 hippocampal neuronal networks than (+)-PCB 95. Interestingly, racemic PCB 95 showed a greater
411 effect on these endpoints than pure PCB 95 atropisomers. (-)-PCB 84 increased the [^{3}H]-phorbol ester
412 binding in rat cerebellar granule cell; however, (-)-PCB 84 and (+)-PCB 84 similarly inhibited uptake of
413 $^{45}Ca^{2+}$ by microsomes isolated from adult rat cerebellum (Lehmler et al., 2005). (+)-PCB 136 showed
414 significant estrogenic activity toward estrogen receptor (ER), whereas (-)-PCB 136 displayed anti-
415 estrogenic activity (Pencikova et al., 2018). A recent *in vivo* study showed that PCB 91 stereoselectively
416 induced oxidative stress in adult zebrafish (Chai et al., 2016). While limited, these studies demonstrate

that the atropisomeric enrichment of neurotoxic PCBs in the environment, wildlife and humans likely has toxicological implications that warrant further investigation.

Like the parent PCBs, OH-PCBs are present in rain and snow, sludge, atmosphere, sediment and soil (Kania-Korwel and Lehmler, 2016a; Tehrani and Van Aken, 2014). They are formed by oxidative processes in living organisms and have been detected in wildlife, including mammals, fish and invertebrates, and in plants (Kania-Korwel and Lehmler, 2016a; Tehrani and Van Aken, 2014). *In vitro* metabolism and animal studies demonstrate that chiral OH-PCBs are formed atropselectively in a congener and species-dependent manner from chiral and prochiral PCB congeners. Chiral OH-PCBs are present in the developing brain of mice exposed developmentally to racemic PCBs (Kania-Korwel et al., 2017); however, the levels, profiles and chiral signatures of these chiral PCB metabolites in the human brain have not been reported to date (Vetter, 2016). Because the position of the OH-group has a profound effect on the interaction of OH-PCBs with cellular targets implicated in PCB neurotoxicity (Kodavanti et al., 2003; Niknam et al., 2013), further studies are needed to determine how differences in OH-PCB metabolite profiles affect neurotoxic outcomes in humans.

Acknowledgments

We thank Drs. S. Joshi, S. Vyas and Y. Song (University of Iowa) for synthesizing the PCB standards and Mr. V. Parcel from the University of Iowa HRMS Facility for help with the GC/TOF-MS analyses.

Funding

This work was supported by the National Institute of Environmental Health Sciences/National Institutes of Health [grant numbers ES05605, ES013661 and ES027169 to HLJ] and the National Science Foundation [CHE-1609669, CHE-1229354 to the MERCURY consortium (http://mercuryconsortium.org/) and CHE-1662030 to EVP]. The content of the manuscript is solely the

442 responsibility of the authors and does not necessarily represent the official views of the National
443 Institute of Environmental Health Sciences or the National Institutes of Health.

444

References

Asher, B.J., D'Agostino, L.A., Way, J.D., Wong, C.S., Harynuk, J.J., 2009. Comparison of peak integration methods for the determination of enantiomeric fraction in environmental samples. Chemosphere 75, 1042-1048.

Bemis, J.C., Seegal, R.F., 2004. PCB-induced inhibition of the vesicular monoamine transporter predicts reductions in synaptosomal dopamine content. Toxicol. Sci. 80, 288-295.

Bordajandi, L.R., Abad, E., Gonzalez, M.J., 2008. Occurrence of PCBs, PCDD/Fs, PBDEs and DDTs in Spanish breast milk: enantiomeric fraction of chiral PCBs. Chemosphere 70, 567-575.

Bucheli, T.D., Brandli, R.C., 2006. Two-dimensional gas chromatography coupled to triple quadrupole mass spectrometry for the unambiguous determination of atropisomeric polychlorinated biphenyls in environmental samples. J. Chromatogr. A 1110, 156-164.

Caudle, W.M., Richardson, J.R., Delea, K.C., Guillot, T.S., Wang, M., Pennell, K.D., Miller, G.W., 2006. Polychlorinated biphenyl–induced reduction of dopamine transporter expression as a precursor to Parkinson's disease–associated dopamine toxicity. Toxicol. Sci. 92, 490-499.

Chai, T., Cui, F., Mu, X., Yang, Y., Qi, S., Zhu, L., Wang, C., Qiu, J., 2016. Stereoselective induction by 2,2',3,4',6-pentachlorobiphenyl in adult zebrafish (*Danio rerio*): Implication of chirality in oxidative stress and bioaccumulation. Environ. Pollut. 215, 66-76.

Chen, S.J., Tian, M., Zheng, J., Zhu, Z.C., Luo, Y., Luo, X.J., Mai, B.X., 2014. Elevated levels of polychlorinated biphenyls in plants, air, and soils at an E-waste site in Southern China and enantioselective biotransformation of chiral PCBs in plants. Environ. Sci. Technol. 48, 3847-3855.

Chu, S., Covaci, A., Schepens, P., 2003. Levels and chiral signatures of persistent organochlorine pollutants in human tissues from Belgium. Environ. Res. 93, 167-176.

European Commission, 2002. Commission decision EC 2002/657 of 12 August 2002 implementing Council Directive 96/23/EC concerning the performance of analytical methods and the interpretation of results, Off. J. Eur. Communities: Legis.

DeCaprio, A.P., Johnson, G.W., Tarbell, A.M., Carpenter, D.O., Chiarenzelli, J.R., Morse, G.S., Santiago-Rivera, A.L., Schymura, M.J., Akwesasne Task Force on the Environment, 2005. Polychlorinated biphenyl (PCB) exposure assessment by multivariate statistical analysis of serum congener profiles in an adult Native American population. Environ. Res. 98, 284-302.

Enayah, S.H., Vanle, B.C., Fuortes, L.J., Doorn, J.A., Ludewig, G., 2018. PCB95 and PCB153 change dopamine levels and turn-over in PC12 cells. Toxicology 394, 93-101.

Feng, W., Zheng, J., Robin, G., Dong, Y., Ichikawa, M., Inoue, Y., Mori, T., Nakano, T., Pessah, I.N., 2017. Enantioselectivity of 2,2',3,5',6-pentachlorobiphenyl (PCB 95) atropisomers toward ryanodine receptors (RyRs) and their influences on hippocampal neuronal networks. Environ. Sci. Technol. 51, 14406-14416.

Forgue, S.T., Allen, J.R., 1982. Identification of an arene oxide metabolite of 2,2',5,5'-tetrachlorobiphenyl by gas chromatography-mass spectroscopy. Chem. Biol. Interact. 40, 233-245.

Forgue, S.T., Preston, B.D., Hargraves, W.A., Reich, I.L., Allen, J.R., 1979. Direct evidence that an arene oxide is a metabolic intermediate of 2,2',5,5'-tetrachlorobiphenyl. Biochem. Biophys. Res. Commun. 91, 475-483.

Frisch, M.J., Trucks, G.W., Schlegel, H.B., Scuseria, G.E., Robb, M.A., Cheeseman, J.R., Scalmani, G., Barone, V., Petersson, G.A., Nakatsuji, H., Li, X., Caricato, M., Marenich, A.V., Bloino, J., Janesko, B.G., Gomperts, R., Mennucci, B., Hratchian, H.P., Ortiz, J.V., Izmaylov, A.F., Sonnenberg, J.L., Williams-Young, D., Ding, F., Lipparini, F., Egidi, F., Goings, J., Peng, B., Petrone, A., Henderson, T., Ranasinghe, D., Zakrzewski, V.G., Gao, J., Rega, N., Zheng, G., Liang, W., Hada, M., Ehara, M., Toyota, K., Fukuda, R., Hasegawa, J., Ishida, M., Nakajima, T., Honda, Y., Kitao, O., Nakai, H., Vreven, T., Throssell, K., Montgomery, J.A., Jr., Peralta, J.E., Ogliaro, F., Bearpark, M.J., Heyd, J.J., Brothers, E.N., Kudin, K.N., Staroverov, V.N., Keith, T.A., Kobayashi, R., Normand, J., Raghavachari, K., Rendell, A.P., Burant, J.C., Iyengar, S.S., Tomasi, J., Cossi, M., Millam, J.M.,

494 Klene, M., Adamo, C., Cammi, R., Ochterski, J.W., Martin, R.L., Morokuma, K., Farkas, O.,
495 Foresman, J.B., Fox, D.J., 2016. Gaussian 16, revision A. 03. Gaussian Inc., Wallingford, CT.
496 Gährs, M., Roos, R., Andersson, P.L., Schrenk, D., 2013. Role of the nuclear xenobiotic receptors CAR
497 and PXR in induction of cytochromes P450 by non-dioxinlike polychlorinated biphenyls in cultured
498 rat hepatocytes. Toxicol. Appl. Pharmacol. 272, 77-85.
499 Glausch, A., Hahn, J., Schurig, V., 1995. Enantioselective determination of chiral 2,2',3,3',4,6'-
500 hexachlorobiphenyl (PCB 132) in human milk samples by multidimensional gas
501 chromatography/electron capture detection and by mass spectrometry. Chemosphere 30, 2079-2085.
502 Grimm, F.A., Hu, D., Kania-Korwel, I., Lehmler, H.J., Ludewig, G., Hornbuckle, K.C., Duffel, M.W.,
503 Bergman, A., Robertson, L.W., 2015. Metabolism and metabolites of polychlorinated biphenyls.
504 Crit. Rev. Toxicol. 45, 245-272.
505 Guengerich, F.P., 2015. Human cytochrome P450 enzymes, in: Ortiz de Montellano, P.R. (Ed.),
506 Cytochrome P450. Springer International Publishing, Cham, pp. 523-785.
507 Guroff, G., Daly, J.W., Jerina, D.M., Renson, J., Witkop, B., Udenfriend, S., 1967. Hydroxylation-
508 induced migration: the NIH shift. Recent experiments reveal an unexpected and general result of
509 enzymatic hydroxylation of aromatic compounds. Science 157, 1524-1530.
510 Haglund, P., Wiberg, K., 1996. Determination of the gas chromatographic elution sequences of the (+)
511 and (-) enantiomers of stable enantiomeric PCBs on Chirasil-Dex. J. High Resol. Chromatogr. 19,
512 373-376.
513 Haijima, A., Lesmana, R., Shimokawa, N., Amano, I., Takatsuru, Y., Koibuchi, N., 2017. Differential
514 neurotoxic effects of in utero and lactational exposure to hydroxylated polychlorinated biphenyl
515 (OH-PCB 106) on spontaneous locomotor activity and motor coordination in young adult male
516 mice. J. Toxicol. Sci. 42, 407-416.

517 Haraguchi, K., Kato, Y., Koga, N., Degawa, M., 2004. Metabolism of polychlorinated biphenyls by
518 Gunn rats: Identification and serum retention of catechol metabolites. Chem. Res. Toxicol. 17, 1684-
519 1691.
520 Haraguchi, K., Koga, N., Kato, Y., 2005. Comparative metabolism of polychlorinated biphenyls and
521 tissue distribution of persistent metabolites in rats, hamsters, and Guinea pigs. Drug Metab. Dispos.
522 33, 373-380.
523 Harrad, S., Ren, J., Hazrati, S., Robson, M., 2006. Chiral signatures of PCB#s 95 and 149 in indoor air,
524 grass, duplicate diets and human faeces. Chemosphere 63, 1368-1376.
525 Hatcher-Martin, J.M., Gearing, M., Steenland, K., Levey, A.I., Miller, G.W., Pennell, K.D., 2012.
526 Association between polychlorinated biphenyls and Parkinson's disease neuropathology.
527 Neurotoxicology 33, 1298-1304.
528 Herrick, R.F., Stewart, J.H., Allen, J.G., 2016. Review of PCBs in US schools: a brief history, an
529 estimate of the number of impacted schools, and an approach for evaluating indoor air samples.
530 Environ. Sci. Pollut. Res. Int. 23, 1975-1985.
531 Jones, D.C., Miller, G.W., 2008. The effects of environmental neurotoxicants on the dopaminergic
532 system: a possible role in drug addiction. Biochem. Pharmacol. 76, 569-581.
533 Jursa, S., Chovancova, J., Petrik, J., Loksa, J., 2006. Dioxin-like and non-dioxin-like PCBs in human
534 serum of Slovak population. Chemosphere 64, 686-691.
535 Kaminsky, L.S., Kennedy, M.W., Adams, S.M., Guengerich, F.P., 1981. Metabolism of
536 dichlorobiphenyls by highly purified isozymes of rat liver cytochrome P-450. Biochemistry 20,
537 7379-7384.
538 Kania-Korwel, I., Duffel, M.W., Lehmler, H.J., 2011. Gas chromatographic analysis with chiral
539 cyclodextrin phases reveals the enantioselective formation of hydroxylated polychlorinated
540 biphenyls by rat liver microsomes. Environ. Sci. Technol. 45, 9590-9596.

541 Kania-Korwel, I., El-Komy, M.H., Veng-Pedersen, P., Lehmler, H.J., 2010. Clearance of
542 polychlorinated biphenyl atropisomers is enantioselective in female C57Bl/6 mice. Environ. Sci.
543 Technol. 44, 2828-2835.
544 Kania-Korwel, I., Hornbuckle, K.C., Peck, A., Ludewig, G., Robertson, L.W., Sulkowski, W.W.,
545 Espandiari, P., Gairola, C.G., Lehmler, H.J., 2005. Congener-specific tissue distribution of Aroclor
546 1254 and a highly chlorinated environmental PCB mixture in rats. Environ. Sci. Technol. 39, 3513-
547 3520.
548 Kania-Korwel, I., Lehmler, H.J., 2016a. Chiral polychlorinated biphenyls: absorption, metabolism and
549 excretion--a review. Environ. Sci. Pollut. Res. Int. 23, 2042-2057.
550 Kania-Korwel, I., Lehmler, H.J., 2016b. Toxicokinetics of chiral polychlorinated biphenyls across
551 different species--a review. Environ. Sci. Pollut. Res. Int. 23, 2058-2080.
552 Kania-Korwel, I., Lukasiewicz, T., Barnhart, C.D., Stamou, M., Chung, H., Kelly, K.M., Bandiera, S.,
553 Lein, P.J., Lehmler, H.J., 2017. Editor's highlight: Congener-specific disposition of chiral
554 polychlorinated biphenyls in lactating mice and their offspring: implications for PCB developmental
555 neurotoxicity. Toxicol. Sci. 158, 101-115.
556 Kania-Korwel, I., Shaikh, N.S., Hornbuckle, K.C., Robertson, L.W., Lehmler, H.J., 2007.
557 Enantioselective disposition of PCB 136 (2,2',3,3',6,6'-hexachlorobiphenyl) in C57BL/6 mice after
558 oral and intraperitoneal administration. Chirality 19, 56-66.
559 Kania-Korwel, I., Zhao, H., Norstrom, K., Li, X., Hornbuckle, K.C., Lehmler, H.J., 2008. Simultaneous
560 extraction and clean-up of polychlorinated biphenyls and their metabolites from small tissue samples
561 using pressurized liquid extraction. J. Chromatogr. A 1214, 37-46.
562 Kannan, N., Reusch, T.B., Schulz-Bull, D.E., Petrick, G., Duinker, J.C., 1995. Chlorobiphenyls: model
563 compounds for metabolism in food chain organisms and their potential use as ecotoxicological stress
564 indicators by application of the metabolic slope concept. Environ. Sci. Technol. 29, 1851-1859.

565 Kennedy, M.W., Carpentier, N.K., Dymerski, P.P., Kaminsky, L.S., 1981. Metabolism of
566 dichlorobiphenyls by hepatic microsomal cytochrome P-450. Biochem. Pharmacol. 30, 577-588.
567 Kodavanti, P.R., Curras-Collazo, M.C., 2010. Neuroendocrine actions of organohalogens: thyroid
568 hormones, arginine vasopressin, and neuroplasticity. Front. Neuroendocrinol. 31, 479-496.
569 Kodavanti, P.R., Ward, T.R., Derr-Yellin, E.C., McKinney, J.D., Tilson, H.A., 2003. Increased
570 [^{3}H]Phorbol Ester Binding in Rat Cerebellar Granule Cells and Inhibition of $^{45}Ca^{2+}$ Buffering in Rat
571 Cerebellum by Hydroxylated Polychlorinated Biphenyls. Neurotoxicology 24, 187-198.
572 Lehmler, H.J., Harrad, S.J., Huhnerfuss, H., Kania-Korwel, I., Lee, C.M., Lu, Z., Wong, C.S., 2010.
573 Chiral polychlorinated biphenyl transport, metabolism, and distribution: a review. Environ. Sci.
574 Technol. 44, 2757-2766.
575 Lehmler, H.J., Robertson, L.W., Garrison, A.W., Kodavanti, P.R., 2005. Effects of PCB 84 enantiomers
576 on [^{3}H]-phorbol ester binding in rat cerebellar granule cells and $^{45}Ca^{2+}$-uptake in rat cerebellum.
577 Toxicol. Lett. 156, 391-400.
578 Lesmana, R., Shimokawa, N., Takatsuru, Y., Iwasaki, T., Koibuchi, N., 2014. Lactational exposure to
579 hydroxylated polychlorinated biphenyl (OH-PCB 106) causes hyperactivity in male rat pups by
580 aberrant increase in dopamine and its receptor. Environ. Toxicol. 29, 876-883.
581 Lu, Z., Kania-Korwel, I., Lehmler, H.-J., Wong, C.S., 2013. Stereoselective formation of mono- and di-
582 hydroxylated polychlorinated biphenyls by rat cytochrome P450 2B1. Environ. Sci. Technol. 47,
583 12184-12192.
584 Marenich, A.V., Cramer, C.J., Truhlar, D.G., 2009. Performance of SM6, SM8, and SMD on the
585 SAMPL1 test set for the prediction of small-molecule solvation free energies. J. Phys. Chem. B 113,
586 4538-4543.
587 Mariussen, E., Fonnum, F., 2001. The effect of polychlorinated biphenyls on the high affinity uptake of
588 the neurotransmitters, dopamine, serotonin, glutamate and GABA, into rat brain synaptosomes.
589 Toxicology 159, 11-21.

590 Mariussen, E., Fonnum, F., 2006. Neurochemical targets and behavioral effects of organohalogen
591 compounds: an update. Crit. Rev. Toxicol. 36, 253-289.
592 McGraw, J.E., Sr., Waller, D.P., 2006. Specific human CYP 450 isoform metabolism of a
593 pentachlorobiphenyl (PCB-IUPAC# 101). Biochem. Biophys. Res. Commun. 344, 129-133.
594 Milanowski, B., Lulek, J., Lehmler, H.J., Kania-Korwel, I., 2010. Assessment of the disposition of
595 chiral polychlorinated biphenyls in female mdr 1a/b knockout versus wild-type mice using
596 multivariate analyses. Environ. Int. 36, 884-892.
597 Nagayoshi, H., Kakimoto, K., Konishi, Y., Kajimura, K., Nakano, T., 2018. Determination of the human
598 cytochrome P450 monooxygenase catalyzing the enantioselective oxidation of 2,2',3,5',6-
599 pentachlorobiphenyl (PCB 95) and 2,2',3,4,4',5',6-heptachlorobiphenyl (PCB 183). Environ. Sci.
600 Pollut. Res. Int. 25, 16420-16426.
601 Niknam, Y., Feng, W., Cherednichenko, G., Dong, Y., Joshi, S.N., Vyas, S.M., Lehmler, H.J., Pessah,
602 I.N., 2013. Structure-activity relationship of selected meta- and para-hydroxylated non-dioxin like
603 polychlorinated biphenyls: from single RyR1 channels to muscle dysfunction. Toxicol. Sci. 136,
604 500-513.
605 Norstroem, K., Bergman, A., 2006. Chiral PCB methyl sulfones and their metabolic formation.
606 Organohalogen Compd. 68, 21-24.
607 Norstrom, K., Eriksson, J., Haglund, J., Silvari, V., Bergman, A., 2006. Enantioselective formation of
608 methyl sulfone metabolites of 2,2',3,3',4,6'-hexachlorobiphenyl in rat. Environ. Sci. Technol. 40,
609 7649-7655.
610 Ohta, C., Haraguchi, K., Kato, Y., Endo, T., Koga, N., 2012. Involvement of rat CYP3A enzymes in the
611 metabolism of 2,2',3,4',5',6-hexachlorobiphenyl (CB149). Organohalogen Compd. 74, 1475-1478.
612 Parkinson, A., Safe, S.H., Robertson, L.W., Thomas, P.E., Ryan, D.E., Reik, L.M., Levin, W., 1983.
613 Immunochemical quantitation of cytochrome P-450 isozymes and epoxide hydrolase in liver

614 microsomes from polychlorinated or polybrominated biphenyl-treated rats. A study of structure-
615 activity relationships. J. Biol. Chem. 258, 5967-5976.
616 Pencikova, K., Brenerova, P., Svrzkova, L., Hruba, E., Palkova, L., Vondracek, J., Lehmler, H.J.,
617 Machala, M., 2018. Atropisomers of 2,2',3,3',6,6'-hexachlorobiphenyl (PCB 136) exhibit
618 stereoselective effects on activation of nuclear receptors in vitro. Environ. Sci. Pollut. Res. Int. 25,
619 16411-16419.
620 Pessah, I.N., Cherednichenko, G., Lein, P.J., 2010. Minding the calcium store: Ryanodine receptor
621 activation as a convergent mechanism of PCB toxicity. Pharmacol. Ther. 125, 260-285.
622 Peverati, R., Truhlar, D.G., 2011. Improving the Accuracy of Hybrid Meta-GGA Density Functionals
623 by Range Separation. The Journal of Physical Chemistry Letters 2, 2810-2817.
624 Preston, B.D., Miller, J.A., Miller, E.C., 1983. Non-arene oxide aromatic ring hydroxylation of 2,2',5,5'-
625 tetrachlorobiphenyl as the major metabolic pathway catalyzed by phenobarbital-induced rat liver
626 microsomes. J. Biol. Chem. 258, 8304-8311.
627 Püttmann, M., Arand, M., Oesch, F., Mannschreck, A., Robertson, L., 1990. Chirality and the induction
628 of xenobiotic-metabolizing enzymes: Effects of the atropisomers of the polychlorinated biphenyl
629 2,2′,3,4,4′,6-hexachlorobiphenyl, in: Frank, H., Holmstedt, B., Testa, B. (Eds.), Chirality and
630 Biological Activity. Alan R. Liss, Inc., New York, pp. 177-184.
631 Püttmann, M., Mannschreck, A., Oesch, F., Robertson, L., 1989. Chiral effects in the induction of drug-
632 metabolizing enzymes using synthetic atropisomers of polychlorinated biphenyls (PCBs). Biochem.
633 Pharmacol. 38, 1345-1352.
634 Richardson, J.R., Miller, G.W., 2004. Acute exposure to aroclor 1016 or 1260 differentially affects
635 dopamine transporter and vesicular monoamine transporter 2 levels. Toxicol. Lett. 148, 29-40.
636 Rodman, L.E., Shedlofsky, S.I., Mannschreck, A., Püttmann, M., Swim, A.T., Robertson, L.W., 1991.
637 Differential potency of atropisomers of polychlorinated biphenyls on cytochrome P450 induction

638 and uroporphyrin accumulation in the chick embryo hepatocyte culture. Biochem. Pharmacol. 41,
639 915-922.
640 Safe, S., Bandiera, S., Sawyer, T., Robertson, L., Safe, L., Parkinson, A., Thomas, P.E., Ryan, D.E.,
641 Reik, L.M., Levin, W., et al., 1985. PCBs: structure-function relationships and mechanism of action.
642 Environ. Health Perspect. 60, 47-56.
643 Schecter, A., Colacino, J., Haffner, D., Patel, K., Opel, M., Papke, O., Birnbaum, L., 2010.
644 Perfluorinated compounds, polychlorinated biphenyls, and organochlorine pesticide contamination
645 in composite food samples from Dallas, Texas, USA. Environ. Health Perspect. 118, 796-802.
646 Schnellmann, R.G., Putnam, C.W., Sipes, I.G., 1983. Metabolism of 2,2',3,3',6,6'-hexachlorobiphenyl
647 and 2,2',4,4',5,5'-hexachlorobiphenyl by human hepatic microsomes. Biochem. Pharmacol. 32,
648 3233-3239.
649 Seegal, R.F., 1996. Epidemiological and laboratory evidence of PCB induced neurotoxicity. Crit. Rev.
650 Toxicol. 26, 709-737.
651 Su, G., Liu, X., Gao, Z., Xian, Q., Feng, J., Zhang, X., Giesy, J.P., Wei, S., Liu, H., Yu, H., 2012.
652 Dietary intake of polybrominated diphenyl ethers (PBDEs) and polychlorinated biphenyls (PCBs)
653 from fish and meat by residents of Nanjing, China. Environ. Int. 42, 138-143.
654 Tehrani, R., Van Aken, B., 2014. Hydroxylated polychlorinated biphenyls in the environment: sources,
655 fate, and toxicities. Environ. Sci. Pollut. Res. Int. 21, 6334-6345.
656 Thomas, K., Xue, J., Williams, R., Jones, P., Whitaker, D., 2012. Polychlorinated biphenyls (PCBs) in
657 school buildings: Sources, environmental levels, and exposures. United States Environmental
658 Protection Agency, Office of Research and Development, National Exposure Research Laboratory.
659 Uwimana, E., Li, X., Lehmler, H.J., 2016. 2,2',3,5',6-Pentachlorobiphenyl (PCB 95) is atropselectively
660 metabolized to para hydroxylated metabolites by human liver microsomes. Chem. Res. Toxicol. 29,
661 2108-2110.

662 Uwimana, E., Li, X., Lehmler, H.J., 2018. Human liver microsomes atropselectively metabolize
663 2,2',3,4',6-pentachlorobiphenyl (PCB 91) to a 1,2-shift product as the major metabolite. Environ.
664 Sci. Technol. 52, 6000-6008.
665 Uwimana, E., Maiers, A., Li, X., Lehmler, H.J., 2017. Microsomal metabolism of prochiral
666 polychlorinated biphenyls results in the enantioselective formation of chiral metabolites. Environ.
667 Sci. Technol. 51, 1820-1829.
668 Vetter, W., 2016. Gas chromatographic enantiomer separation of polychlorinated biphenyls (PCBs):
669 Methods, metabolisms, enantiomeric composition in environmental samples and their interpretation.
670 Isr. J. Chem. 56, 940-957.
671 Voorspoels, S., Covaci, A., Neels, H., 2008. Dietary PCB intake in Belgium. Environ. Toxicol.
672 Pharmacol. 25, 179-182.
673 Waller, S.C., He, Y.A., Harlow, G.R., He, Y.Q., Mash, E.A., Halpert, J.R., 1999. 2,2',3,3',6,6'-
674 Hexachlorobiphenyl hydroxylation by active site mutants of cytochrome P450 2B1 and 2B11.
675 Chem. Res. Toxicol. 12, 690-699.
676 Warner, N.A., Martin, J.W., Wong, C.S., 2009. Chiral polychlorinated biphenyls are biotransformed
677 enantioselectively by mammalian cytochrome P-450 isozymes to form hydroxylated metabolites.
678 Environ. Sci. Technol. 43, 114-121.
679 Weigend, F., Ahlrichs, R., 2005. Balanced basis sets of split valence, triple zeta valence and quadruple
680 zeta valence quality for H to Rn: Design and assessment of accuracy. Phys. Chem. Chem. Phys. 7,
681 3297-3305.
682 Whitcomb, B.W., Schisterman, E.F., Buck, G.M., Weiner, J.M., Greizerstein, H., Kostyniak, P.J., 2005.
683 Relative concentrations of organochlorines in adipose tissue and serum among reproductive age
684 women. Environ. Toxicol. Pharmacol. 19, 203-213.

685 Wong, C.S., Garrison, A.W., Smith, P.D., Foreman, W.T., 2001. Enantiomeric composition of chiral
686 polychlorinated biphenyl atropisomers in aquatic and riparian biota. Environ. Sci. Technol. 35,
687 2448-2454.
688 Wu, X., Duffel, M., Lehmler, H.J., 2013a. Oxidation of polychlorinated biphenyls by liver tissue slices
689 from phenobarbital-pretreated mice is congener-specific and atropselective. Chem. Res. Toxicol. 26,
690 1642-1651.
691 Wu, X., Kammerer, A., Lehmler, H.J., 2014. Microsomal oxidation of 2,2',3,3',6,6'-hexachlorobiphenyl
692 (PCB 136) results in species-dependent chiral signatures of the hydroxylated metabolites. Environ.
693 Sci. Technol. 48, 2436-2444.
694 Wu, X., Kania-Korwel, I., Chen, H., Stamou, M., Dammanahalli, K.J., Duffel, M., Lein, P.J., Lehmler,
695 H.J., 2013b. Metabolism of 2,2',3,3',6,6'-hexachlorobiphenyl (PCB 136) atropisomers in tissue slices
696 from phenobarbital or dexamethasone-induced rats is sex-dependent. Xenobiotica 43, 933-947.
697 Wu, X., Lehmler, H.J., 2016. Effects of thiol antioxidants on the atropselective oxidation of
698 2,2',3,3',6,6'-hexachlorobiphenyl (PCB 136) by rat liver microsomes. Environ. Sci. Pollut. Res. Int.
699 23, 2081-2088.
700 Wu, X., Pramanik, A., Duffel, M.W., Hrycay, E.G., Bandiera, S.M., Lehmler, H.J., Kania-Korwel, I.,
701 2011. 2,2',3,3',6,6'-Hexachlorobiphenyl (PCB 136) is enantioselectively oxidized to hydroxylated
702 metabolites by rat liver microsomes. Chem. Res. Toxicol. 24, 2249-2257.
703 Yang, D., Kania-Korwel, I., Ghogha, A., Chen, H., Stamou, M., Bose, D.D., Pessah, I.N., Lehmler, H.J.,
704 Lein, P.J., 2014. PCB 136 atropselectively alters morphometric and functional parameters of
705 neuronal connectivity in cultured rat hippocampal neurons via ryanodine receptor-dependent
706 mechanisms. Toxicol. Sci. 138, 379-392.
707 Zheng, J., Yan, X., Chen, S.J., Peng, X.W., Hu, G.C., Chen, K.H., Luo, X.J., Mai, B.X., Yang, Z.Y.,
708 2013. Polychlorinated biphenyls in human hair at an e-waste site in China: composition profiles and
709 chiral signatures in comparison to dust. Environ. Int. 54, 128-133.

710 Zheng, J., Yu, L.H., Chen, S.J., Hu, G.C., Chen, K.H., Yan, X., Luo, X.J., Zhang, S., Yu, Y.J., Yang,
711 Z.Y., Mai, B.X., 2016. Polychlorinated biphenyls (PCBs) in human hair and serum from e-waste
712 recycling workers in Southern China: Concentrations, chiral signatures, correlations, and source
713 identification. Environ. Sci. Technol. 50, 1579-1586.

714

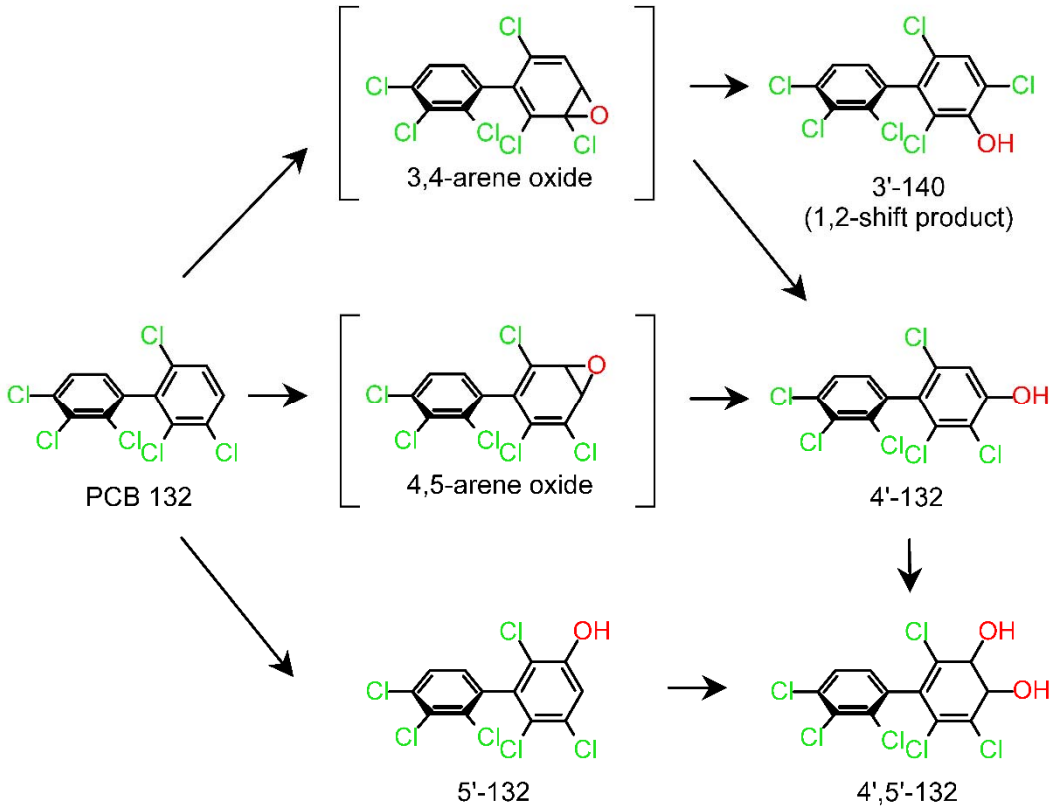

715

716 **Fig. 1.** Proposed metabolism scheme showing the chemical structures of metabolites of racemic PCB
717 132 identified in incubations with HLMs. Only one atropisomer of each metabolite is shown for clarity
718 reasons. Abbreviations: 2,2',3,3',4,6'-hexachlorobiphenyl, PCB 132; 2,2',3,4,4',6'-hexachlorobiphenyl-3-
719 ol, 3'-140; 2,2',3,3',4,6'-hexachlorobiphenyl-4'-ol, 4'-132; 2,2',3,3',4,6'-hexachlorobiphenyl-5'-ol, 5'-132;
720 cytochrome P450 enzymes, P450. The minor dihydroxylated metabolite, 4',5'-132 (4',5'-dihydroxy-
721 2,2',3,3',4,6'-hexachlorobiphenyl), is not shown.

722

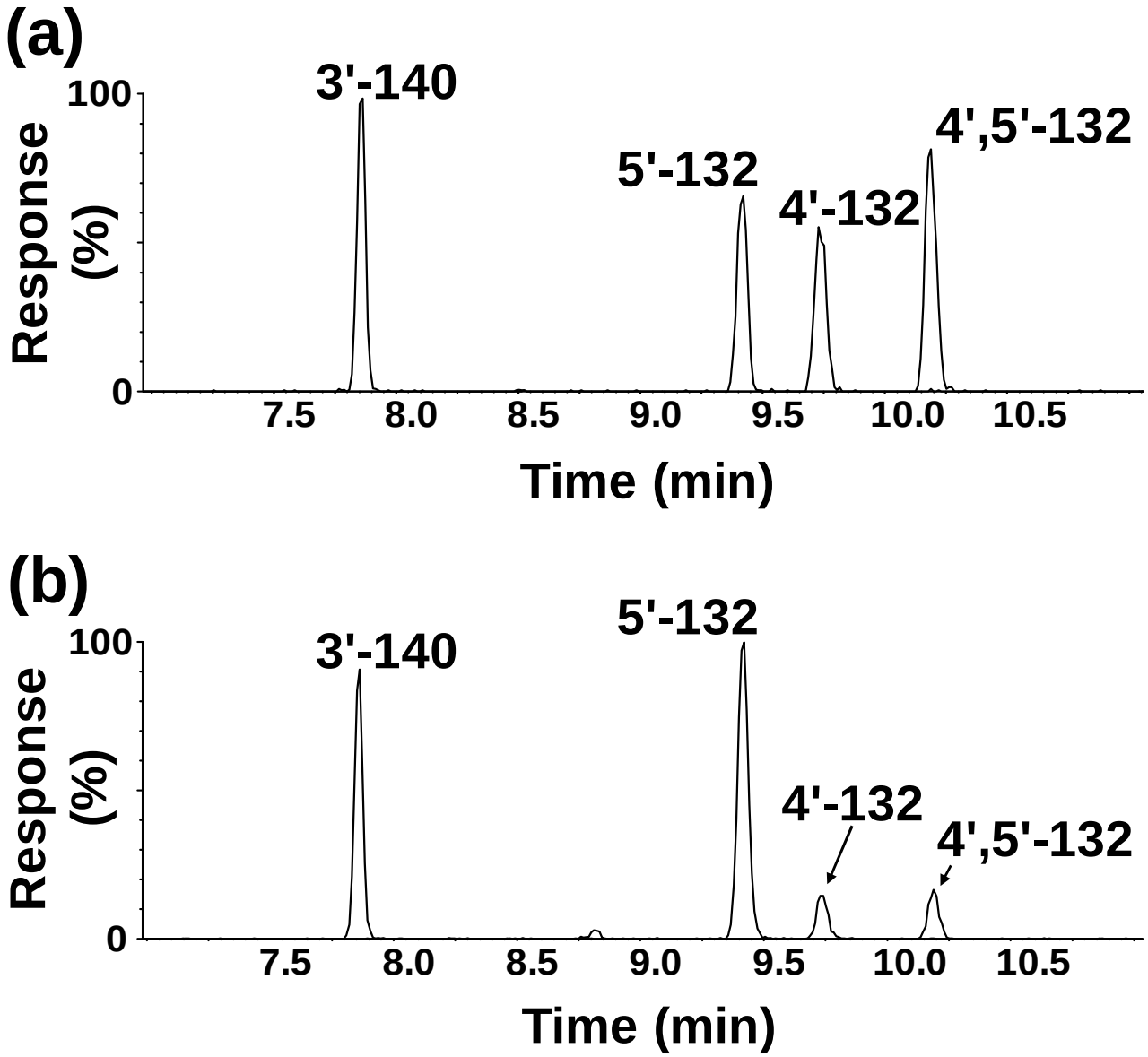

723

724 **Fig. 2. Three monohydroxylated (*m/z* 387.9) and one dihydroxylated (*m/z* 417.9) metabolite were**
725 **identified in incubations of racemic PCB 132 with pHLMs.** Representative gas chromatograms
726 showing (a) the reference standard containing four hydroxylated PCB 132 metabolites and (b) an extract
727 from a representative incubation of racemic PCB 132 with pHLMs. All metabolites were analyzed as
728 the corresponding methylated derivatives. Incubations were carried out with 50 µM racemic PCB 132,
729 0.3 mg/mL microsomal protein and 1 mM NADPH for 90 min at 37 °C. The metabolites were identified

730 based on their retention times relative to the corresponding authentic standard and their *m/z*. For the

731 corresponding mass spectra, see **Figs. S4** to **S11**.

732

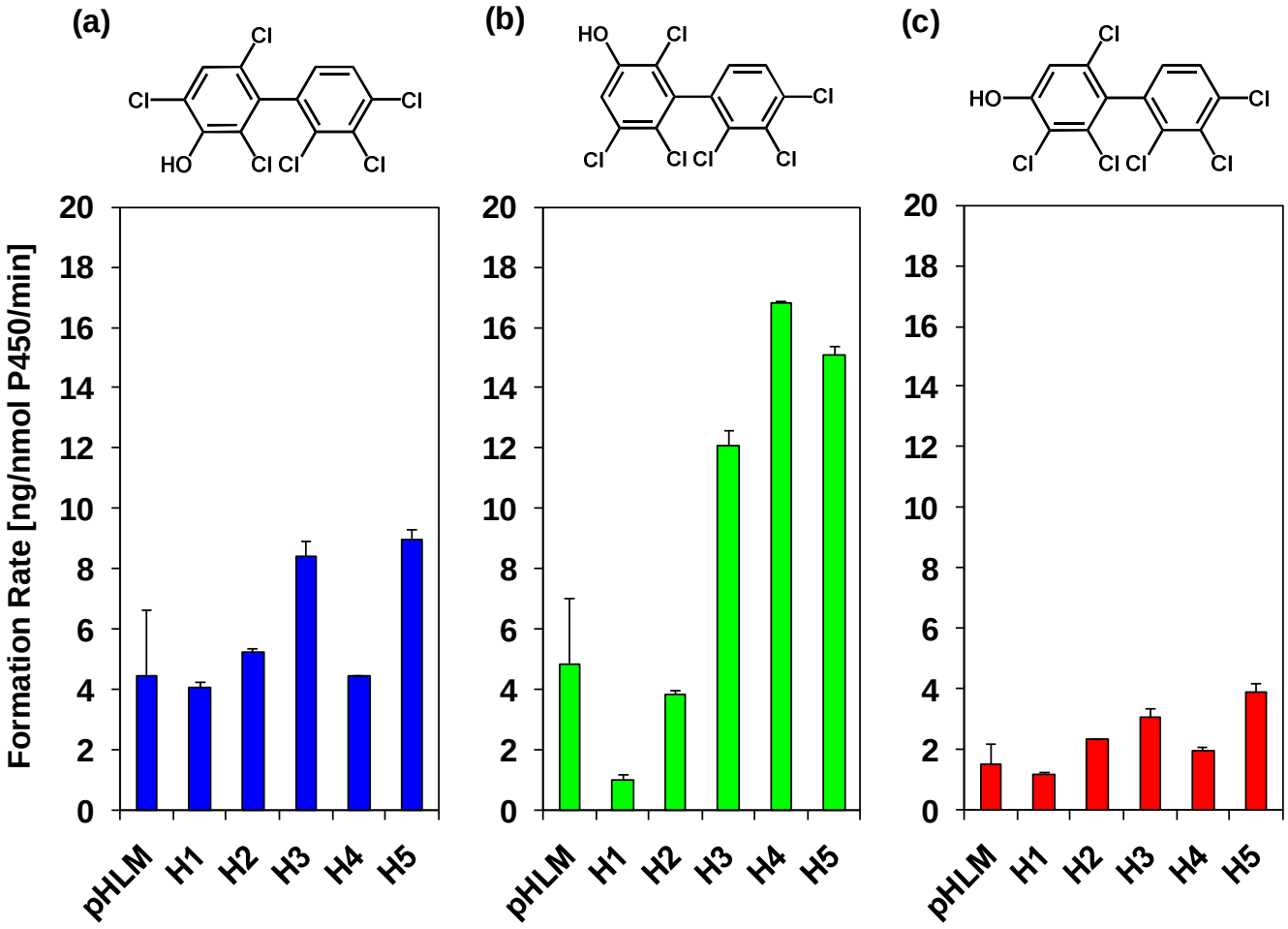

733

734 **Fig. 3. Formation rates of PCB 132 metabolites by different HLM preparations display inter-**
735 **individual differences, with (a) the *meta* hydroxylated metabolites, 3'-140 (1,2- shift product), and**
736 **(b) 5'-132, being major metabolites, and (c) the *para* hydroxylated metabolite, 4'-132, being a**
737 **minor metabolite.** Incubations were carried out with 50 µM racemic PCB 132, 0.1 mg/mL microsomal
738 protein and 1 mM NADPH for 10 min at 37 °C (**Tables S3** and **S4**) as reported earlier (Uwimana et al.,
739 2016, 2018). Extracts from the microsomal incubations were derivatized with diazomethane and
740 analyzed by GC-µECD; see Materials and Methods for additional details. Data are presented as mean ±
741 standard deviation, n = 3.

742

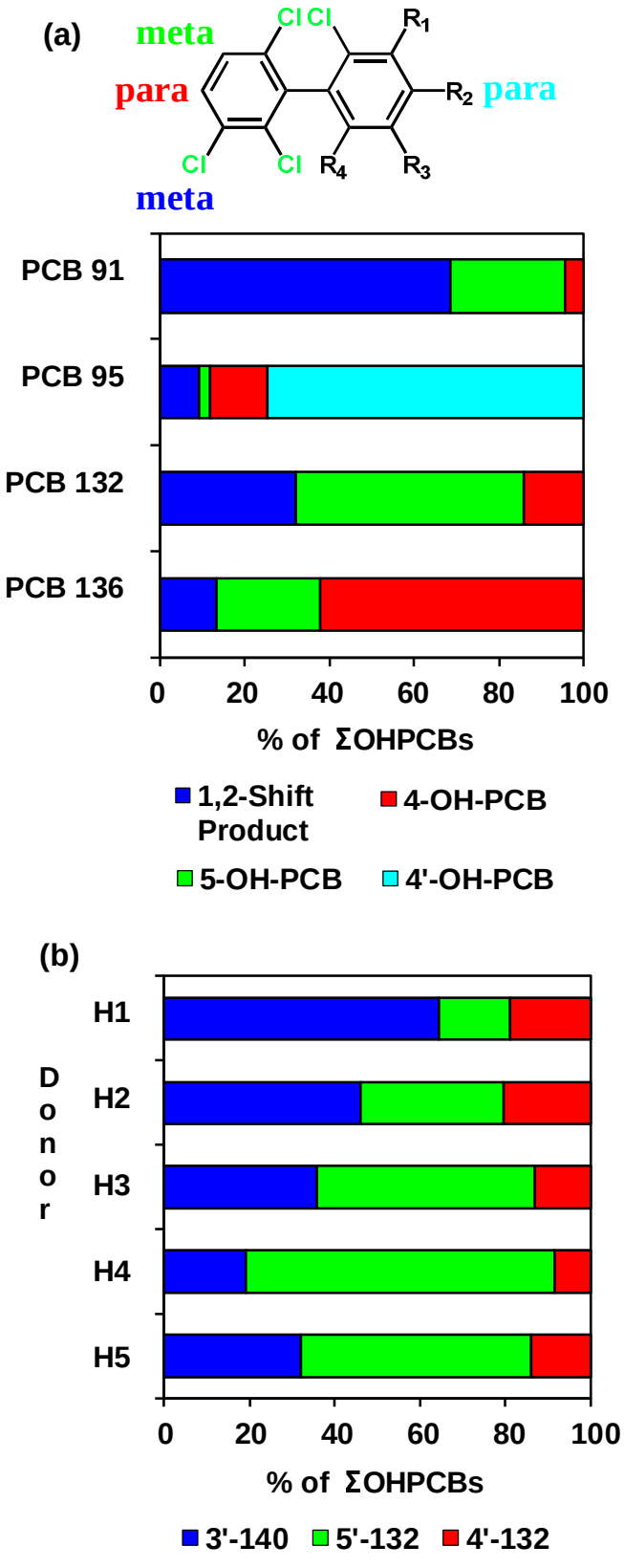

743

744 **Fig. 4. The profile of PCB 132 OH-PCB metabolite formed by pHLMs is (a) distinctively different**

745 **from the published metabolite profiles of structurally related PCB congeners (*i.e.* PCB 91, PCB 95**

and PCB 136) and (b) shows considerable inter individual variability. (a) Bar diagrams comparing the profiles of hydroxylated metabolites of PCB 91, PCB 95, PCB 132 and PCB 136 formed in incubations with pHLMs. PCB 91 (Uwimana et al., 2018) and PCB 132 (this study) are preferentially oxidized in *meta* position, whereas PCB 95 (Uwimana et al., 2016) and PCB 136 (Wu et al., 2014) are hydroxylated in *para* position. In the case of PCB 95, the oxidation occurs preferentially in the *para* position of the lower chlorinated 2,5-dichlorophenyl ring (Uwimana et al., 2016). Incubations were carried out with 50 µM PCB, 0.1 mg/mL microsomal protein and 1 mM NADPH for 5 min (PCB 91 and PCB 95) or 10 min (PCB 132 and PCB 136) at 37 °C using the same pHLM preparation. (b) Bar diagrams showing inter-individual differences in profiles of hydroxylated metabolites of PCB 132 formed in incubations with different single donor HLM preparations. Incubations were carried out with 50 µM PCB 132, 0.1 mg/mL microsomal protein and 1 mM NADPH for 10 min at 37 °C (Uwimana et al., 2016). Extracts from the microsomal incubations were derivatized with diazomethane and analyzed by GC-µECD; see Materials and Methods for additional details.

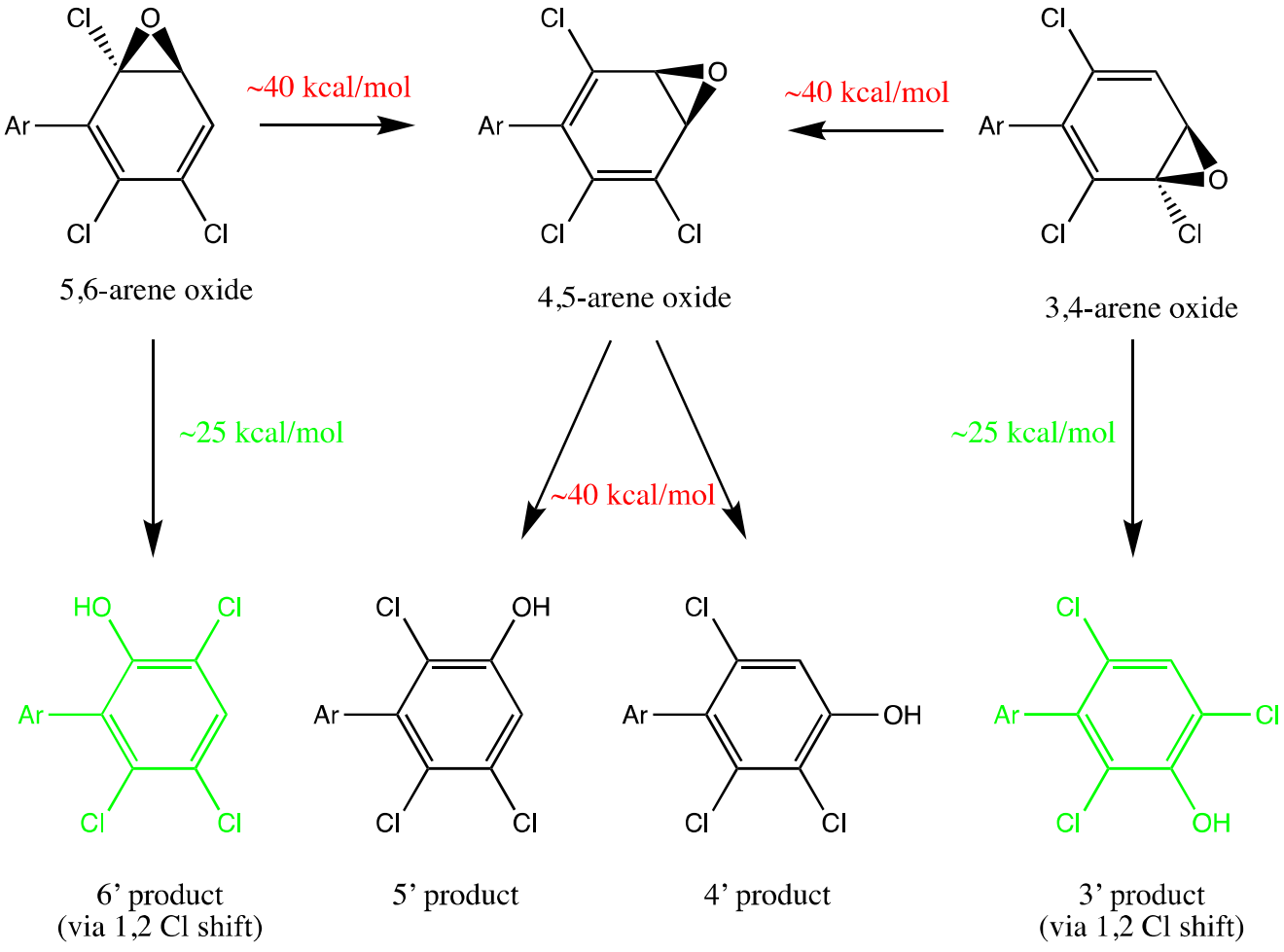

759

760 **Fig. 5. The formation of 1,2 chlorine shift metabolites via arene oxide intermediates of chiral**

761 **PCBs is energetically favored.** Energies shown are free energies of activation at the M11/def2-SVP

762 level of theory with the SMD aqueous continuum solvation model.

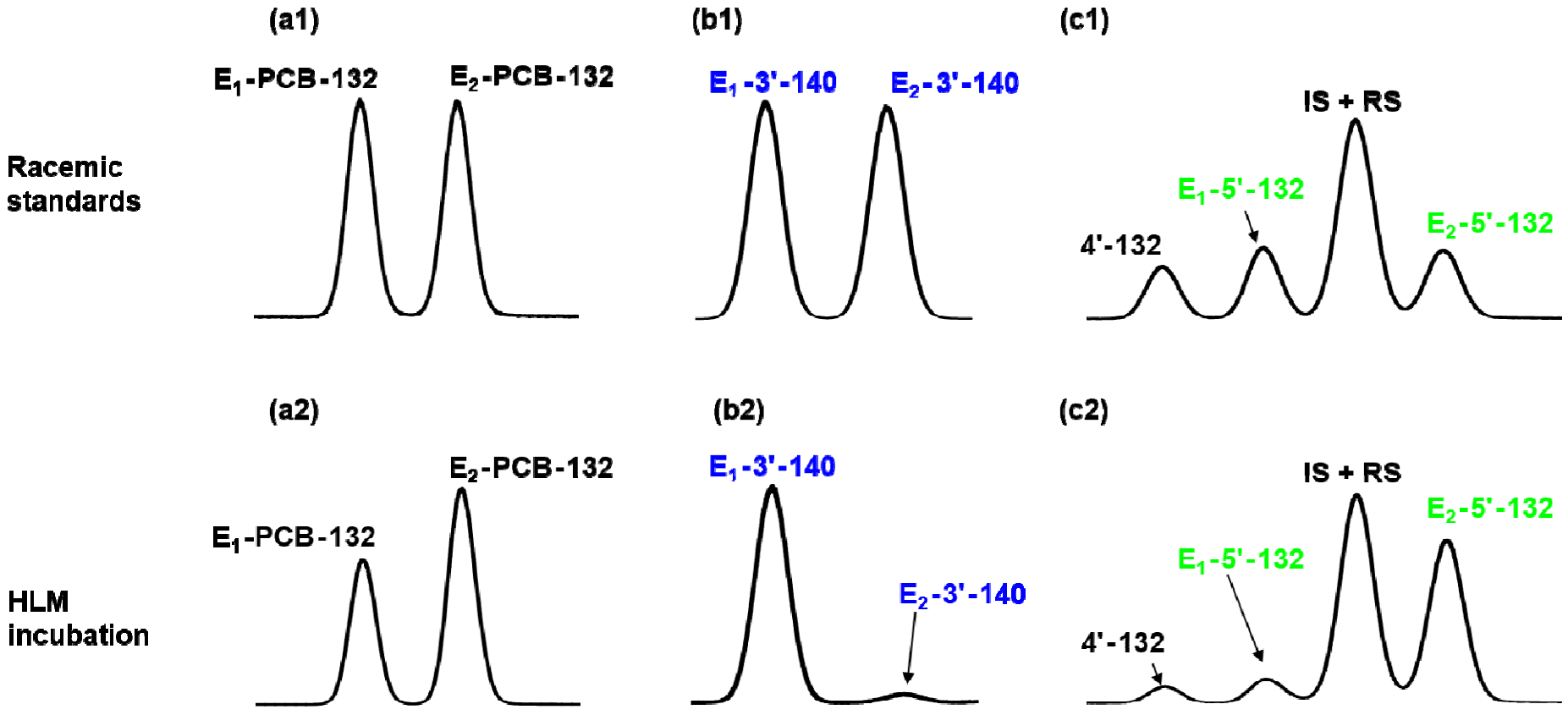

Fig. 6. Atropselective gas chromatographic analysis revealed the atropselective metabolism of racemic PCB 132 to 5'-132 and 3'-140 in incubations with pHLMs. Representative gas chromatograms of racemic standards (top panels) *vs.* PCB 132, 5'-132 and 3'-140 formed in incubations of racemic PCB 132 with HLMs (bottom panels) show a depletion of E_1-PCB 132 (panels a1 *vs.* a2) and atropselective formation of E_1-3'-140 (panels b1 *vs.* b2) and E_2-5'-132 (panels c1 *vs.* c2). To assess the atropselective depletion of PCB 132, incubations were carried out with 5 µM PCB 132, 0.5 mg/mL microsomal protein (pHLMs only) and 0.5 mM NADPH for 120 min at 37 °C. To study the atropselective formation of the PCB 132 metabolites, incubations were carried out with 50 µM racemic PCB 132, 0.1 mg/mL microsomal protein and 1 mM NADPH for 30

min at 37 °C (donor H3 shown here; see Fig. 6 for results from incubations using other human liver microsome preparations) (Uwimana et al., 2016, 2018). Metabolites were analyzed as the corresponding methylated derivatives after derivatization with diazomethane. Atropselective analyses of 3'-140 were performed with a GTA column at 150 °C, and atropselective analyses of PCB 132 and 5'-132 were carried out with a CD column at 160 °C (Kania-Korwel et al., 2011).

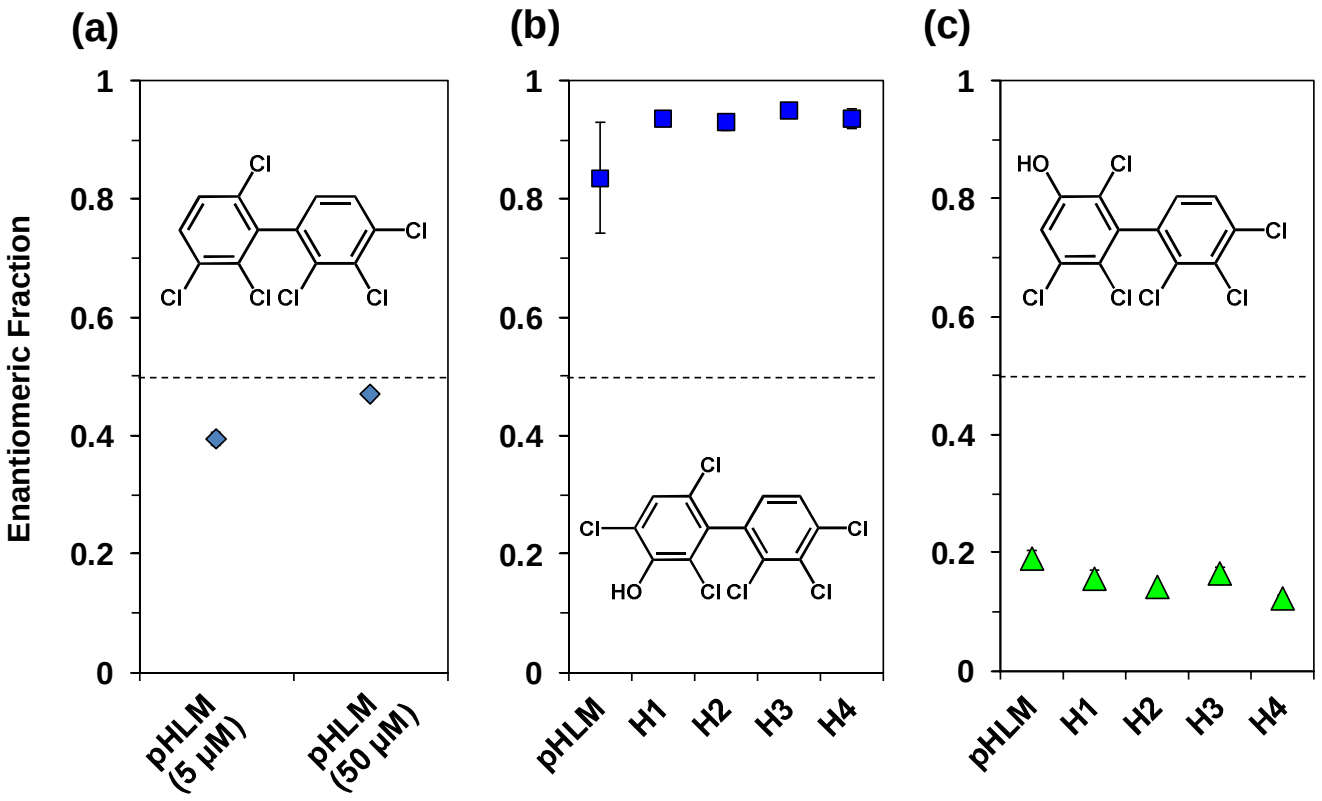

Fig. 7 Enantiomeric fractions (EFs) of (a) parent PCB 132, (b) 3'-140 and (c) 5'-132 reveal only small inter-individual differences in the atropselective formation of both metabolites. (a) To assess the atropselective depletion of PCB 132, incubations were carried out with 5 µM or 50 µM PCB 132, 0.5 mg/mL microsomal protein (using pHLMs only), 0.5 mM NADPH for 120 min at 37 °C (see **Fig. 7d** for a representative chromatogram). To study the atropselective formation of (b) 3'-140 and (c) 5'-132, microsomal incubations were carried out with 50 µM racemic PCB 132, 0.1 mg/mL microsomal protein, 1 mM NADPH for 30 min at 37 °C (Uwimana et al., 2016, 2018). Metabolites were analyzed as the corresponding methylated derivatives. Atropselective analyses of 3'-140 were performed with a GTA column at 150 °C, and atropselective analyses of PCB 132 and 5'-132 were carried out with a CD column at 160°C (Kania-Korwel et al., 2011). EF values could not be determined in incubations with HLMs from donor H5 due to the low metabolite levels. Data are presented as mean ± standard deviation, n = 3. The dotted line indicates the EF values of the racemic standards. * EF values were significantly different from the respective racemic standard (t-test, $p < 0.05$).

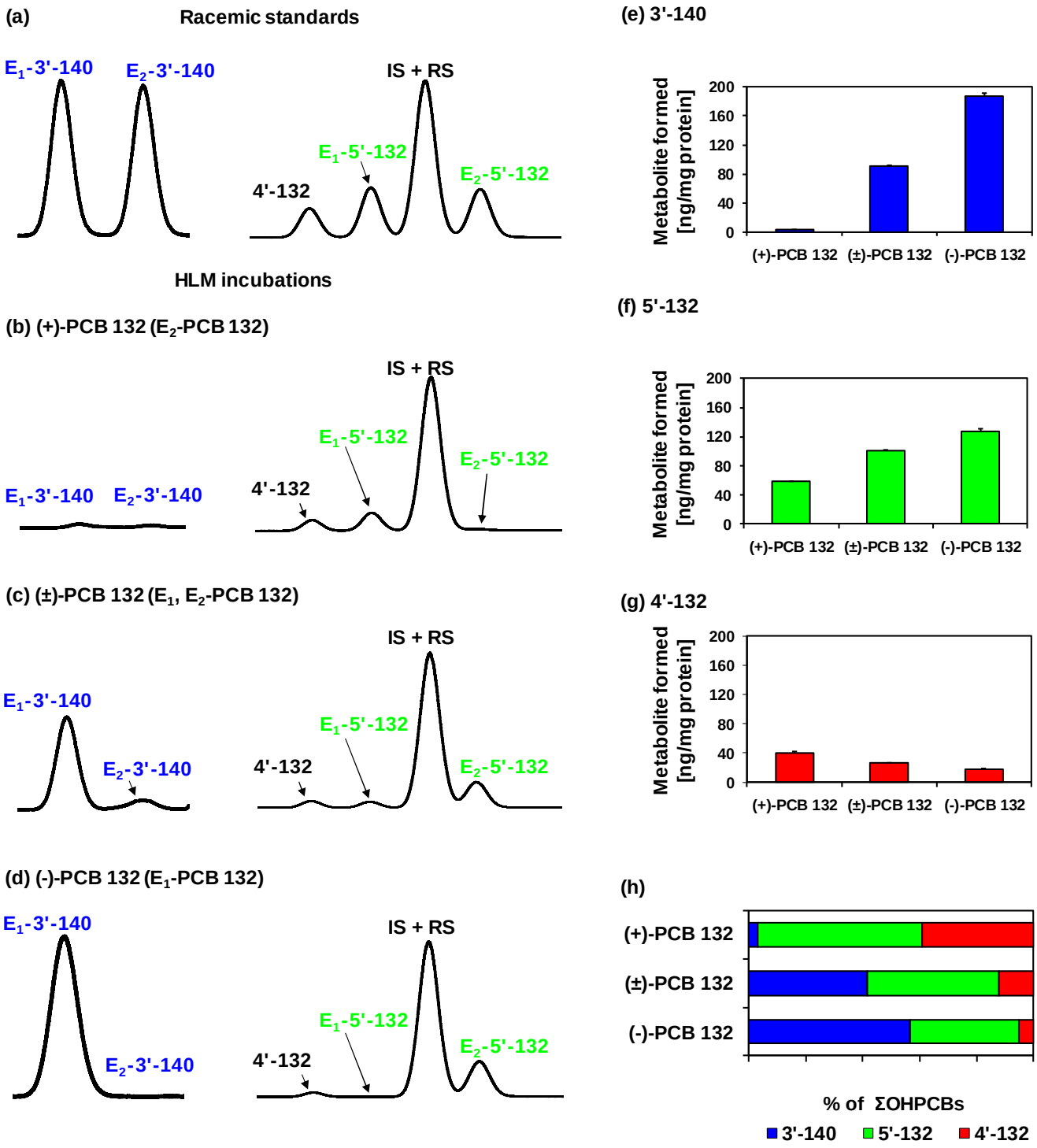

Fig. 8. Comparison of representative gas chromatograms of (a) racemic OH-PCB metabolite standards with OH-PCB metabolites formed in incubations of (b) (+)-PCB 132, (c) (±)-PCB 132 or (d) (-)-PCB 132 with pHLMs reveals that E_1-5'-132 is formed from (+)-PCB 132 and E_1-3'-140, and E_2-5'-132 are formed from (-)-PCB. Moreover, (e) 3'-140 and (f) 5'-132, but not (g) 4'-132 are formed more rapidly from (-)-PCB 132 than (+)-PCB 132, resulting (h) in distinct OH-PCB

metabolite profiles formed from (+)-, (±)-, and (-)-PCB 132 in incubations with pHLMs.

Incubations were carried out with 50 µM (+)-PCB 132, racemic PCB 132 or (-)-PCB 132, 0.1 mg/mL microsomal protein and 1 mM NADPH for 30 min at 37 °C (Uwimana et al., 2016). Metabolites were analyzed as the corresponding methylated derivatives after derivatization with diazomethane. Atropselective analyses of 3'-140 were performed with a GTA column at 150 °C, and atropselective analyses of PCB 132 and 5'-132 were carried out with a CD column at 160°C. 4'-132 was not resolved on any of the columns used in this study (Kania-Korwel et al., 2011).